SAFETY WINDOW SHIELD TO PROTECT AGAINST EXTERNAL EXPLOSIONS

by

R. L. Shope and W. A. Keenan
Naval Civil Engineering Laboratory
Port Hueneme, CA 93043

Prepared for Twenty-Fourth DOD Explosives Safety Seminar
Adam's Mark Hotel, St. Louis, Missouri

28-30 August 1990

ABSTRACT

This paper describes the conceptual design, predicted performance, and development plan for a new design concept being developed by the Naval Civil Engineering Laboratory for safety windows in both new and existing buildings. The concept, named the safety window shield, protects the building interior against effects from accidental explosions outside the building, including blast overpressures, fragments, and debris. Instead of transferring window loads to the exterior wall, the shield transfers the applied window loads to the wall-ceiling and wall-floor joints where the building is inherently strong. This vastly reduces collateral building damage and the probability of structural collapse from an explosion. The acquisition, installation, and maintenance costs make the shield an economical, reliable, and effective way to increase the safety of personnel in buildings from accidental explosions associated with ammunition logistics.

The design concept is a polycarbonate shield mounted in a steel frame suspended immediately behind the window opening from steel cables connected to the ceiling and floor. Energy absorbers and lead mass concealed inside the frame control dynamic response of the shield to an explosion. The cables restrain the shield in a blocking position behind the window opening to protect the building interior during the critical time when blast overpressures, casing fragments, glass shards, and debris act on the window.

Report Documentation Page

Form Approved
OMB No. 0704-0188

1. REPORT DATE	2. REPORT TYPE	3. DATES COVERED
AUG 1990		**00-00-1990 to 00-00-1990**

4. TITLE AND SUBTITLE	5a. CONTRACT NUMBER
Safety Window Shield to Protect Against External Explosions	5b. GRANT NUMBER
	5c. PROGRAM ELEMENT NUMBER
6. AUTHOR(S)	5d. PROJECT NUMBER
	5e. TASK NUMBER
	5f. WORK UNIT NUMBER
7. PERFORMING ORGANIZATION NAME(S) AND ADDRESS(ES) **Naval Civil Engineering Laboratory, ,Port Hueneme,CA,93043**	8. PERFORMING ORGANIZATION REPORT NUMBER
9. SPONSORING/MONITORING AGENCY NAME(S) AND ADDRESS(ES)	10. SPONSOR/MONITOR'S ACRONYM(S)
	11. SPONSOR/MONITOR'S REPORT NUMBER(S)

12. DISTRIBUTION/AVAILABILITY STATEMENT
Approved for public release; distribution unlimited

13. SUPPLEMENTARY NOTES
See also ADA235005, Volume 1. Minutes of the Explosives Safety Seminar (24th) Held in St. Louis, MO on 28-30 August 1990.

14. ABSTRACT
see report

15. SUBJECT TERMS

16. SECURITY CLASSIFICATION OF:			17. LIMITATION OF ABSTRACT	18. NUMBER OF PAGES	19a. NAME OF RESPONSIBLE PERSON
a. REPORT **unclassified**	b. ABSTRACT **unclassified**	c. THIS PAGE **unclassified**	**Same as Report (SAR)**	**37**	

1.0 INTRODUCTION

1.1 PROBLEM

Terrorist bombings directed against U.S. facilities and accidental explosions from ammunition logistics have prompted a need for ways to upgrade buildings to protect inhabitants from explosions. Historical records of explosions show that inhabitants are most vulnerable to explosion effects that enter interior spaces through windows, as illustrated in Figure 1-1.

The threats from explosions include blast overpressures, flying debris, glass shards, and fragments entering the building through windows. The concept of a safety window shield evolved as a means to defeat these threats in both new and existing buildings.

The common approach to protect against explosion effects is to install a hardened window and frame. While this approach will protect the building interior, there are several disadvantages. The principal disadvantage is that the blast loads applied to a hardened window are transferred directly to the adjoining wall. This vastly increases collateral damage to unhardened buildings which, in turn, increases the probability of structural collapse. Also, hardened windows are very expensive and time consuming to install, especially in existing buildings. Further, blast hardened windows are permanent modifications which cannot be easily altered to accommodate a change in the threat level. In most buildings, hardened windows provide neither a practical nor affordable solution for life safety.

1.2 SOLUTION

The safety window shield is a polycarbonate panel mounted in a steel frame which is suspended immediately behind the window opening from steel cables connected to the ceiling and floor, as illustrated in Figure 1-2. An explosion outside the building destroys the conventional glass window covering the opening and directly loads the shield. The cables restrain the shield in a blocking position behind the window opening to protect the building interior during the critical time when blast overpressures, casing fragments, glass shards, and debris try to enter through the window openings. Blast, fragment, and debris loads applied to the shield are transferred by the cables to the wall-ceiling and wall-floor joints where buildings are inherently strong. This vastly reduces collateral building damage and the probability of structural collapse from the explosion.

1.3 SCOPE

The safety window shield can be designed to defeat a variety of threats, including blast overpressures from explosions, flying debris and fragments, small arms fire, electronic surveillance, and forced entry. However, this paper deals primarily with the theory and design for a safety window shield to protect interior spaces from external explosions.

(a) No safety window shield

(b) Safety window shield behind each window

Figure 1-1. Life safety in buildings with and without safety window shields.

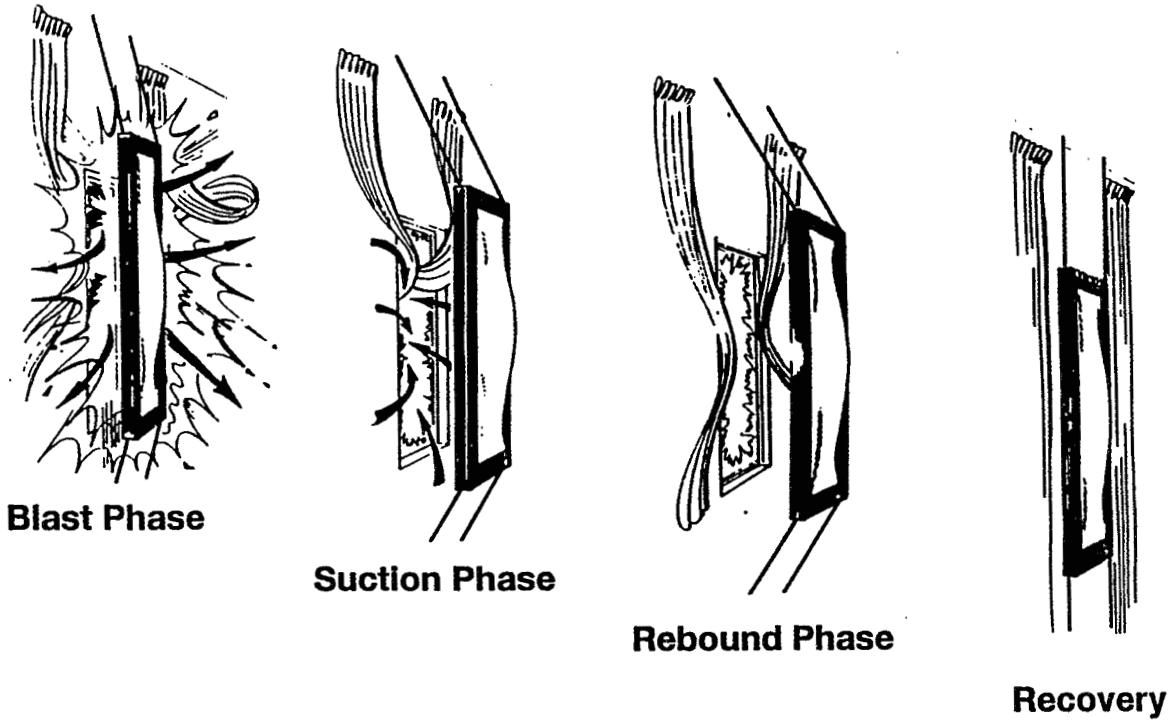

Figure 1-2. Dynamic response of shield to external explosion.

2.0 SAFETY WINDOW SHIELD

2.1 THREAT

The design threat is an explosion outside the building. Design parameters are the TNT equivalent weight of the explosion, the location of the explosion relative to the window opening, and the number, mass, and velocity of fragments and debris striking the window opening.

2.2 FUNCTION

Safety window shields are installed on the interior of the building, directly behind the window openings. The shields block threats from entering the building. A typical safety window shield is shown in Figures 2-1 through 2-8. The major components of the system are a polycarbonate glazing panel, a tubular steel frame that holds the glazing, four cables which suspend the shield behind the window opening, energy absorbers inside the vertical rails of the frame, and lead ballast inside the horizontal rails of the frame.

The safety window shield protects inhabitants by remaining in a blocking position behind the window opening during the critical time when blast overpressures, fragments, and debris try to enter the opening. When an explosion occurs, the shock wave arrives at the building, strikes the window, and reflects back. The result is an instantaneous rise in pressure on the window. This blast load easily fails the window glass and causes the shield to displace horizontally into the room. This movement creates a vent area around the shield for blast pressures to enter the room. However, this vent area is small compared to the area of the window opening. Consequently, the pressures escaping into the room are greatly reduced. In addition to reducing overpressures, the shield acts as a barrier to reduce the number of fragments, debris and glass shards entering the room.

2.3 COMPONENTS

2.3.1 Glazing

The glazing is a thin panel of polycarbonate material, such as Lexan. Both faces of the polycarbonate are covered with a commercial film to inhibit environmental degradation of the glazing. The glazing is mounted in a steel frame and held in place by bolts uniformly spaced along the perimeter of the glazing. The length and width of the glazing are equal to those of the window opening. The stress-strain characteristics of the polycarbonate, shown in Figure 2-6, allow the glazing to absorb the blast energy by work done in the form of strain energy associated with large inelastic deflections of the glazing acting as a tensile membrane.

2.3.2 Frame

The frame supports the polycarbonate glazing and is made up of standard AISC tubing. The horizontal and vertical members of the frame are welded together. A glazing boot made up of steel plates is welded to the tubes to hold the polycarbonate panel in place, as shown in Figure 2-7. The boot is lined with a uroprene gasket that develops friction forces to resist pull-out of the polycarbonate as it undergoes large membrane deflections.

2.3.3 Cables

Four cables hold the shield in position immediately behind the window opening as shown in Figure 2-1. Two cables are connected to the wall-ceiling joint and two cables are connected to the wall-floor joint, as shown in Figure 2-8. The other ends of the cables are attached to the pull-rods in the energy absorbers, as shown in Figure 2-4. The cables are pretensioned to restrain the shield flush against the interior face of the wall. Additional cables can be installed in vertical mullions to accommodate wide windows.

2.3.4 Energy Absorbers

Four energy absorbers are concealed inside the steel frame tubing, one near each end of the two vertical rails, as shown in Figures 2-2 and 2-3. The energy absorber is a series of aluminum honeycomb blocks threaded onto a steel rod. Each block is sandwiched between a steel bearing plate and a steel resisting plate. The bearing plates are connected by ring keys to the rod. The resisting plates are connected by shear pins to the steel tubing. Tension in the rod causes compression in the honeycomb blocks.

Any shield motions produce tension in the top and bottom cables which, in turn, produces tension in the rod of each energy absorber. Significant shield motions produce cable tension forces sufficient to crush the honeycomb blocks.

A typical stress-strain curve for the aluminum honeycomb material is shown in Figure 2-5. This material can be obtained with crushing strengths ranging from 15 to 10,000 psi. Once the material reaches its crushing strength, it will undergo large inelastic strains with no significant increase in stress until it locks up at strains exceeding 75 percent. It is evident from Figure 2-5 that the crushable material can dissipate a large amount of energy.

2.3.5 Ballast

Ballast, in the form of lead beads, is packed into the space inside the top and bottom horizontal rails of the frame, as shown in Figure 2-7. The lead ballast increases the total mass of the system which, in turn, reduces the horizontal shield displacements, thus reducing the peak blast overpressure inside the room. In addition to reducing shield displacements, the ballast can be proportioned between the top and bottom rails so as to minimize the rigid body rotation of the shield. Reducing the rotation limits the amount of debris allowed to enter the room.

2.3.6 Cable Anchors

The cables are threaded through holes drilled in the floor and ceiling, as illustrated in Figure 2-8. A standard cable connector, such as a lead-filled wedge sleeve, anchors the cable to the back face of the floor and ceiling. A steel anchor plate is used to safely distribute the cable forces into the structural floor/ceiling system. The shield is drawn against the wall by pretensioning the cables before the connectors are fastened to the cables.

2.4 PERFORMANCE OBJECTIVES

The shield design should consider the following performance objectives for life safety of inhabitants:

- Limit the peak incident blast overpressures inside the room
- Limit the number of fragments and debris entering the room
- Limit the maximum horizontal displacement of the shield into the room

Typical safety thresholds are as follows:

- Overpressure. The peak incident blast overpressures inside the room shall not exceed 1.2 psi at a point 8 feet behind the window opening and 5 feet above the floor.
- Fragments. No more than one bomb fragment shall enter the room through the window opening with an energy content exceeding 58 ft-lbs. No debris and glass shards shall perforate the glazing. However, in no case shall the penetration resistance of the glazing be required to exceed that of the adjoining wall.
- Displacements. The maximum horizontal displacement of the shield into the room shall not exceed 12 inches.

2.5 INSTALLATION

2.5.1 Security Film

For maximum shield effectiveness, the glass in the window behind the shield is covered with a thin layer of plastic security film. This film binds the glass shards together, thereby reducing the number and lethality of glass shards entering the room.

2.5.2 Air Gap

The effectiveness of the shield in mitigating peak blast overpressures entering the room increases with the air gap distance, defined as the distance from the face of the glass window to the face of the shield. The blast wave must accelerate the mass of the broken window glass and move it through the air-gap distance before the glass shards and trailing blast wave can strike the shield. During this time interval, the blast overpressures outside the building are decaying. This decay reduces the peak blast overpressures trying to enter the room around the shield.

The air gap also serves to prevent degradation of the polycarbonate due to ultra violet rays from sunlight.

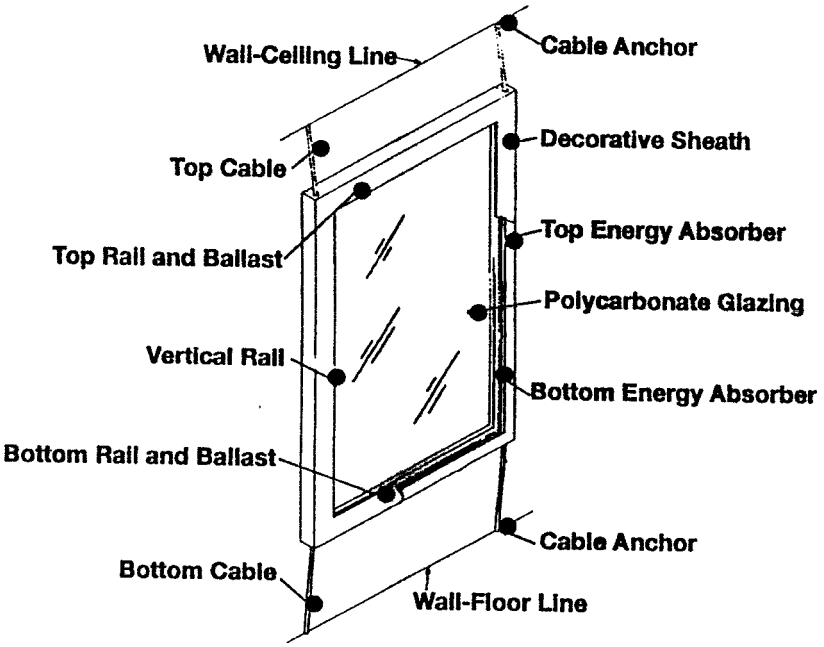

Figure 2-1. Shield components.

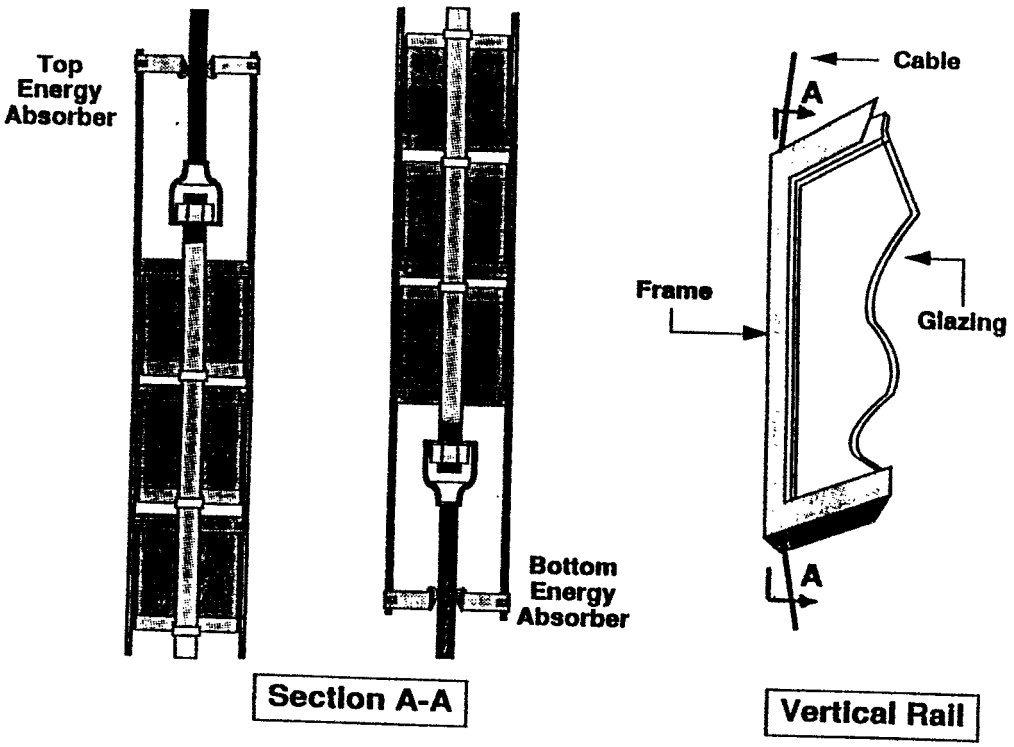

Figure 2-2. Cables and energy absorbers.

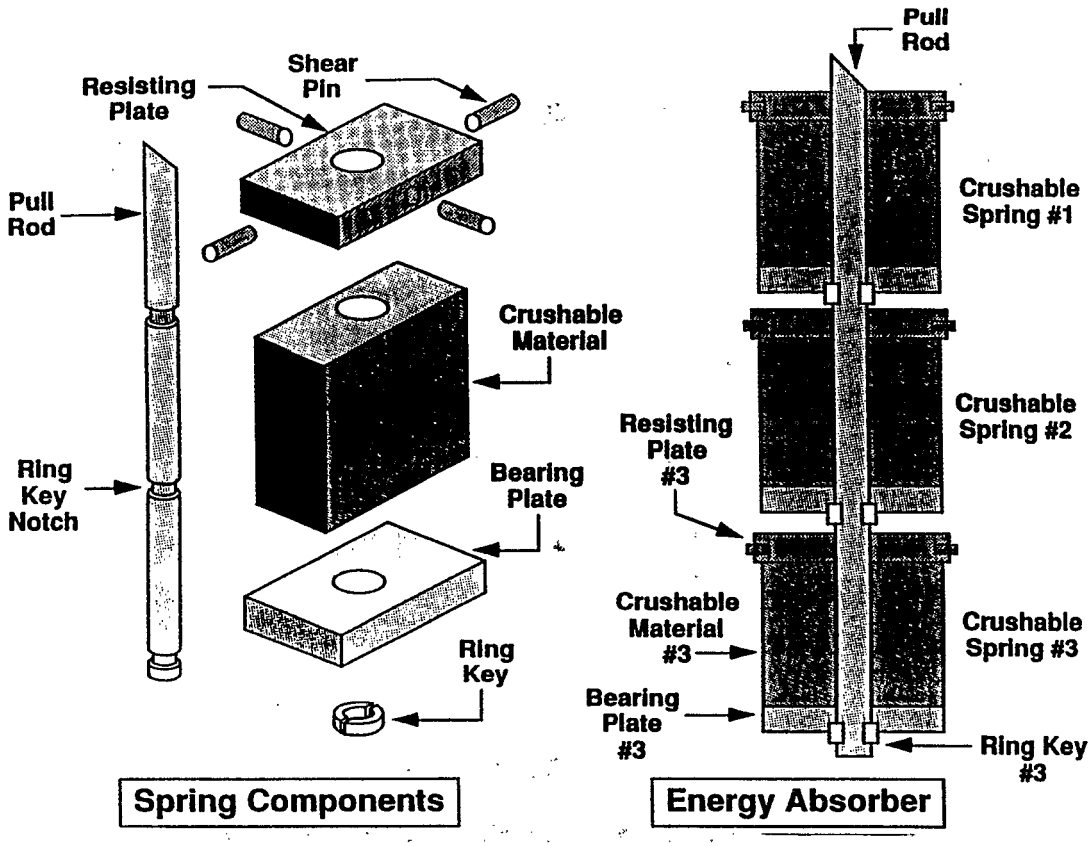

Figure 2-3. Energy absorber components.

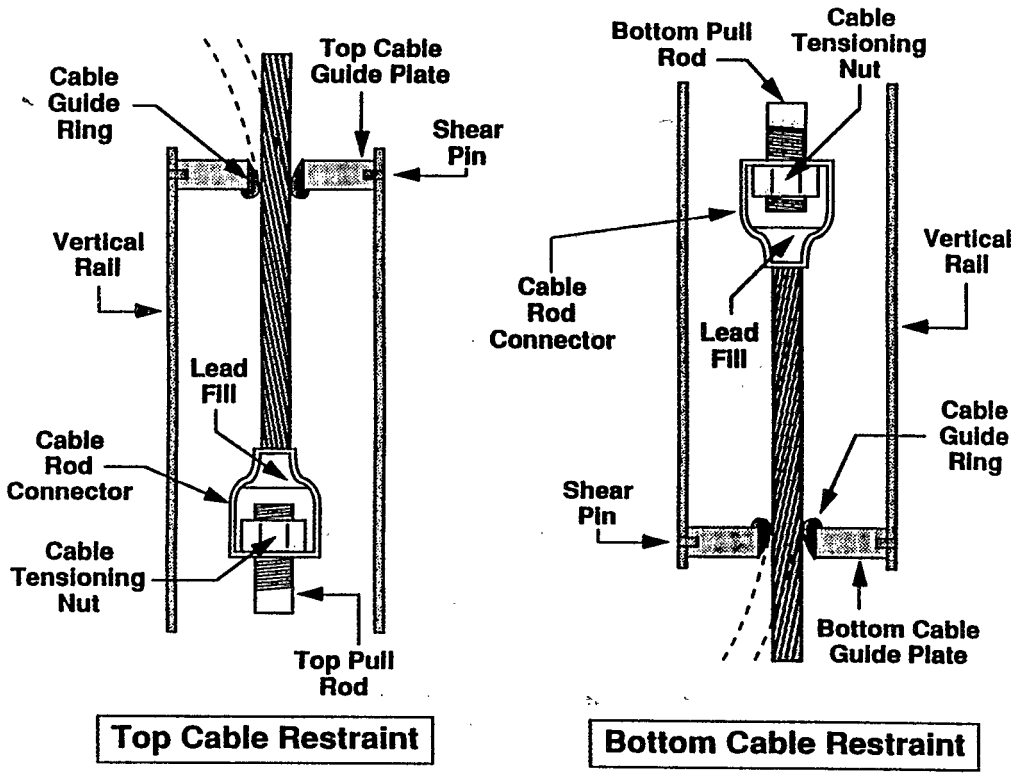

Figure 2-4. Cable restraint system.

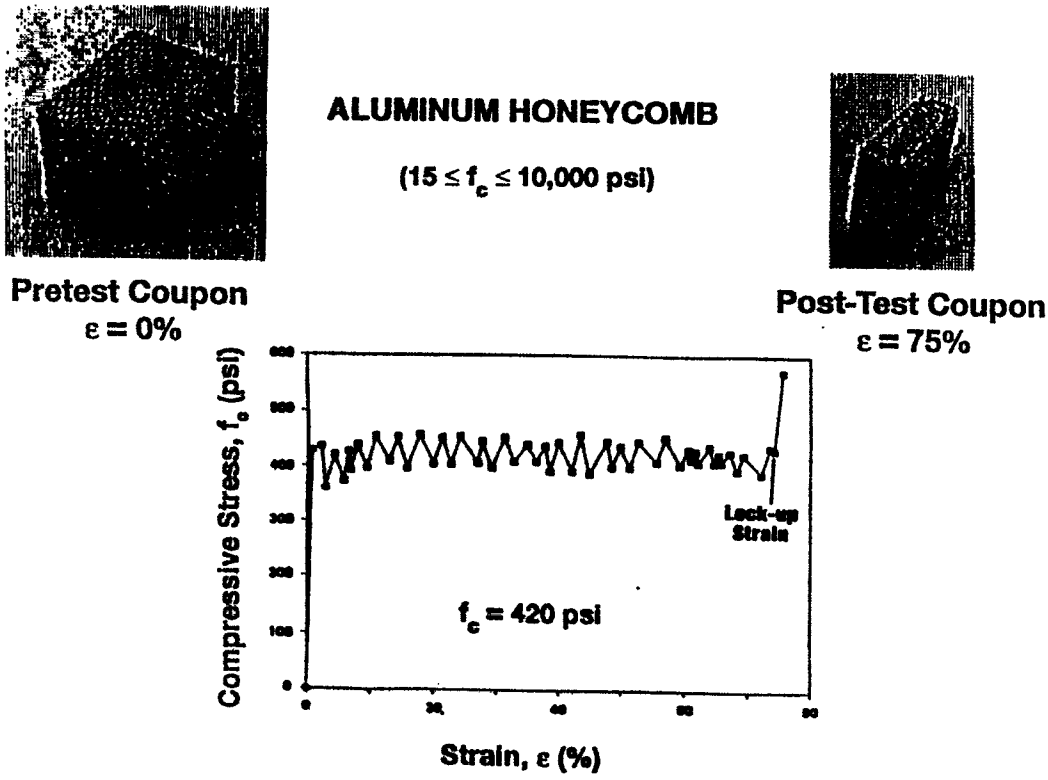

Figure 2-5. Stress-strain characteristics of aluminum honeycomb material.

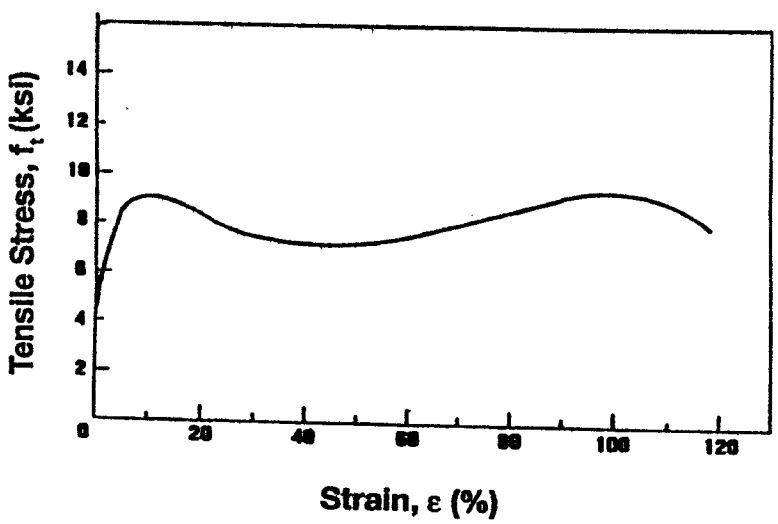

Figure 2-6. Stress-strain characteristics of polycarbonate glazing.

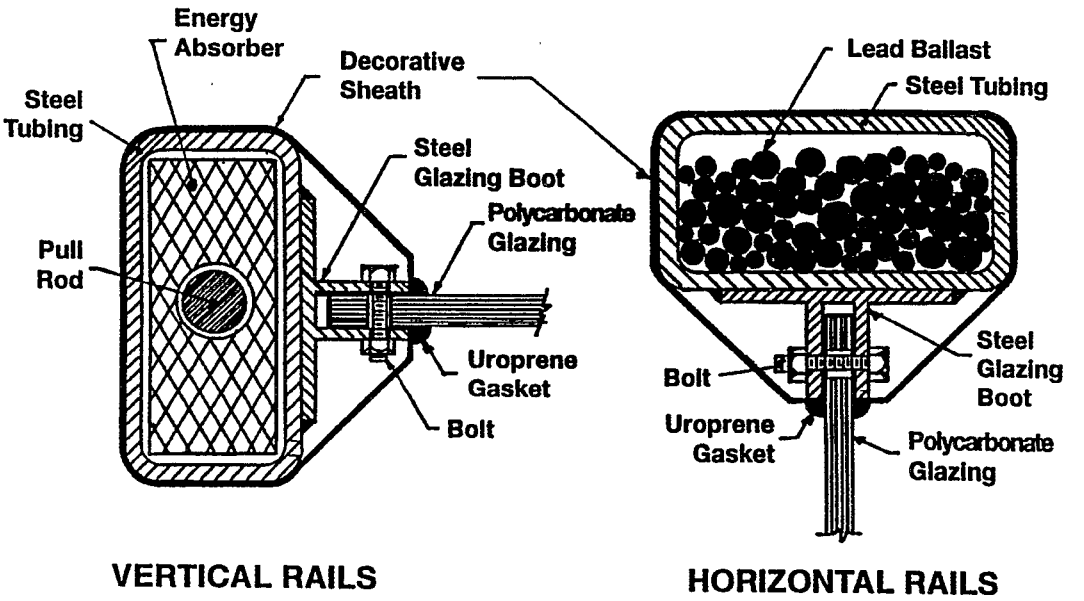

Figure 2-7. Rails, boots, ballast, energy absorbers, and glazing for shield.

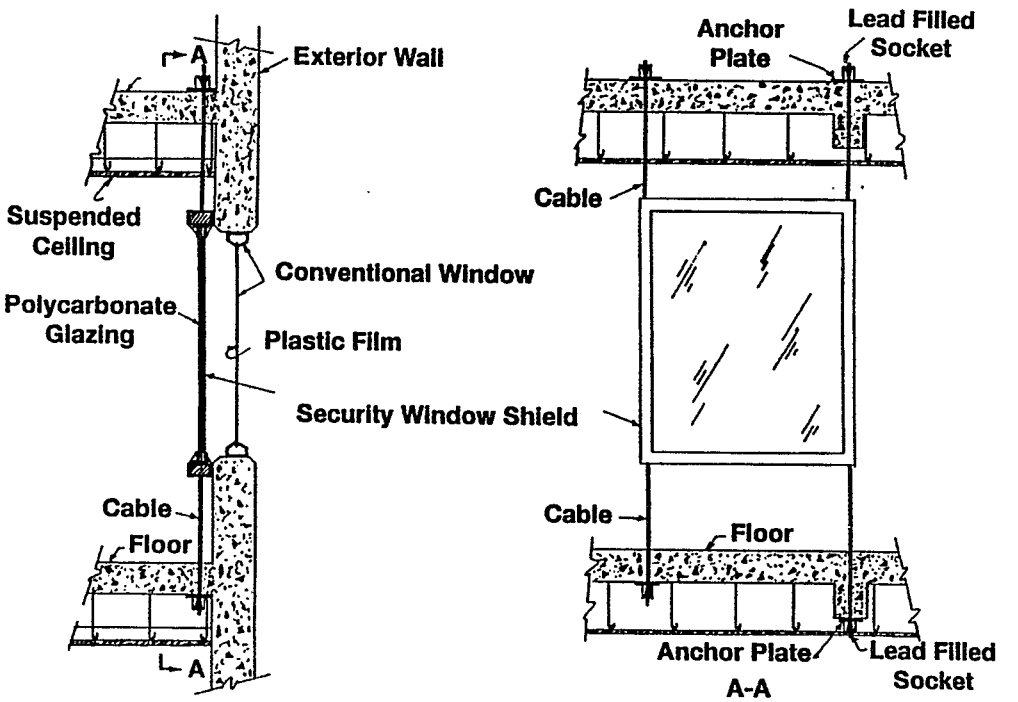

Figure 2-8. Safety window shield installed in reinforced concrete building.

3.0 THEORY

3.1 BLAST OVERPRESSURES

Consider a building subjected to the blast overpressure from a hemispherical, surface burst explosion. The blast overpressure is a function of time, the charge weight, and the standoff distance from the building to the charge. Given the charge weight, W, and the standoff distance, R, the NAVFAC P-397 Manual (Ref 1) can be used to find the peak reflected pressure, P_r, the reflected impulse, i_r, and the positive duration of the pressure, T_o. The time history of the overpressure is defined as follows (Ref 2):

$$P_e(t) = P_r \left(1 - \frac{t}{T_o} \right) e^{-\beta_L t/T_o} \qquad (3.1)$$

Equation (3.1) is plotted in Figure 3-1.

The decay factor, β_L, in equation (3.1) is a constant. The value of β_L depends on the reflected impulse, i_R, which is the area under the pressure-time curve shown in Figure 3-1 or:

$$i_r = \int_{t=0}^{t=T_o} P_e(t)\, dt$$

Substituting equation 3.1 and solving for β_L,

$$\beta_L = \left[\frac{P_r T_o}{i_r} \left(e^{-\beta_L} + \beta_L - 1 \right) \right]^{1/2}$$

Rearranging terms,

$$C_1 \beta_L^2 - e^{-\beta_L} - \beta_L + 1 = 0 \qquad (3.2)$$

where $C_1 = \dfrac{i_r}{P_r T_o}$

The Bisection method (Ref 3) is used to solve equation (3.2). It can be shown that for the possible range of C_1, the value of β_L will range from 0 to 50. Thus, the Bisection method of root solving should be implemented over a range of β_L from 0 to 50 where there is only one root other than the trivial root at $\beta_L = 0$.

3.2 DISPLACEMENTS

3.2.1 Window Glass

In most cases, the shield will be installed behind an existing glass window with an air gap between the glass and the polycarbonate. The glass will have little resistance to the blast overpressures. Therefore, this resistance is assumed to be zero, regardless of the glass thickness. However, the glass will have significant mass such that at any time t,

$$P_e(t) = m_{G1}\, a_{G1}(t)$$

where $P_e(t)$ = external blast overpressure applied to the glass, psi

m_{G1} = unit mass of the glass panel, lb-msec^2/in^3

$a_{G1}(t)$ = acceleration of the glass at time t, in/msec^2

Substituting equation (3.1) for $P_e(t)$,

$$a_{G1}(t) = \frac{P_r}{m_{G1}} \left(1 - \frac{t}{T_o} \right) e^{-\beta_L t/T_o} \qquad (3.3)$$

By integrating equation (3.3), the velocity, $V_{G1}(t)$, and displacement, $X_{G1}(t)$, of the glass shards are,

$$V_{G1}(t) = \frac{P_r}{m_{G1}} e^{-\beta_L t/T_o} \left[\frac{-T_o}{\beta_L} + \left(\frac{T_o}{\beta_L^2}\right) \left(\frac{\beta_L\, t}{T_o} + 1\right) \right] + C_2 \qquad (3.4)$$

$$X_{G1}(t) = \frac{P_r\, T_o}{m_{G1}\, \beta_L^2} e^{-\beta_L t/T_o} \left[T_o - t - \frac{2\, T_o}{\beta_L} \right] + C_2\, t + C_3 \qquad (3.5)$$

where

$$C_2 = \frac{-P_r}{m_{G1}} \left[\frac{-T_o}{\beta_L} + \frac{T_o}{\beta_L^2} \right]$$

$$C_3 = \frac{-P_r}{m_{G1}} \left[\frac{T_o^2}{\beta_L^2} - \frac{2\, T_o^2}{\beta_L^3} \right]$$

The glass must travel a distance d_{G1} before it strikes the shield. The time required for the glass to impact the shield, t_{im}, can be determined by letting $X_{G1}(t) = d_{G1}$ in equation (3.5) and solving for t_{im}. An effective way to find t_{im} is to repeatedly solve equation (3.5), increasing the value of t each time by adding a small time increment, δt. The procedure is stopped when $X_{G1}(t) \geq d_{G1}$ and the current value of t is taken as t_{im}.

The glass shards strike the shield at time t_{im} and impart an initial velocity, V_i. For conservation of momentum at time $t = t_{im}$,

$$V_i = \frac{W_{G1}\, V_{G1}(t_{im})}{(W_{G1} + W_s)} \qquad (3.6)$$

where W_{G1} = total weight of the glass panel, lb

W_s = total weight of the shield, including frame, energy absorbers, and ballast, lb.

$V_{G1}(t_{im})$ = glass velocity at time t_{im} determined from equation (3.4), in/msec.

3.2.2 Shield

Once the glass shards and trailing blast wave strike the shield, the shield begins to displace into the room. This displacement is assumed to result from rigid body motion of the shield, with no deformation of the steel frame and the polycarbonate glazing. The error associated with this assumption is conservative since plastic deformations in the glazing and frame will absorb additional energy from the blast.

Figure 3-2 shows the shield at some time during the loading phase. At any time, t, the position of the shield can be defined by three variables:

X_G = horizontal displacement of centroid of shield, in.

Y_G = vertical displacement of centroid of shield, in.

α_G = rotation of shield about centroid of shield, radians.

A free body diagram of the shield is shown in Figure 3-3. The forces acting on the shield are the resultant horizontal and vertical pressure forces, $F_h(t)$ and $F_v(t)$, the sum of the forces in the top and bottom cables, T_1 and T_2, the total weight of the shield, W_s, and the ballast in the top and bottom horizontal frame rails W_1 and W_2.

From the free body diagram in Figure 3-3, dynamic equilibrium of the forces require:

For $\Sigma F_x = 0$:

$$m_s \ddot{X}_G = F_h(t) - T_1 \sin\theta - T_2 \sin\beta \tag{3.7}$$

where $F_h(t) = P_e(t)\, A_s \cos\alpha_G$

A_s = Area of shield, in^2

For $\Sigma F_y = 0$:

$$m_s \ddot{Y}_G = F_v(t) + T_1 \cos\theta - T_2 \cos\beta - W_s - W_1 - W_2 \tag{3.8}$$

where $F_v(t) = P_e(t)\, A_s \sin\alpha_G$

For $\Sigma M_G = 0$:

$$I_G \ddot{\alpha}_G = (T_1 \sin\theta) (\frac{h_f}{2} \cos\alpha_G) - (T_1 \cos\theta) (\frac{h_f}{2} \sin\alpha_G)$$

$$- (T_2 \sin\beta) (\frac{h_f}{2} \cos\alpha_G) - (T_2 \cos\beta) (\frac{h_f}{2} \sin\alpha_G)$$

$$+ W_1 (\frac{h_f}{2} \sin\alpha_G) - W_2 (\frac{h_f}{2} \sin\alpha_G) \tag{3.9}$$

where from the displaced geometry shown in Figure 3-2:

$$\sin\theta = \frac{X_{o1} + X_1}{Y_1} = \frac{(X_{o1} + X_1)}{[(X_{o1} + X_1)^2 + K_1^2]^{1/2}} \tag{3.10}$$

$$\cos\theta = \frac{K_1}{Y_1} = \frac{K_1}{[(X_{o1} + X_1)^2 + K_1^2]^{1/2}} \tag{3.11}$$

$$\sin\beta = \frac{X_{o2} + X_2}{Y_2} = \frac{(X_{o2} + X_2)}{[(X_{o2} + X_2)^2 + K_2^2]^{1/2}} \tag{3.12}$$

$$\cos\beta = \frac{K_2}{Y_2} = \frac{K_2}{[(X_{o2} + X_2)^2 + K_2^2]^{1/2}} \tag{3.13}$$

and

$$X_1 = X_G - \frac{h_f}{2} \sin \alpha_G \tag{3.14}$$

$$X_2 = X_G + \frac{h_f}{2} \sin \alpha_G \tag{3.15}$$

$$K_1 = h_1 + \frac{h_f}{2} - \frac{h_f}{2} \cos \alpha_G - Y_G \tag{3.16}$$

$$K_2 = h_2 + \frac{h_f}{2} - \frac{h_f}{2} \cos \alpha_G + Y_G \tag{3.17}$$

Substituting equations (3.10) through (3.17) into equations (3.7) through (3.9) and integrating, expressions are obtained for the shield displacements X_G, Y_G, and α_G.

Now, expressions are needed for the cable forces T_1 and T_2 in terms of X_G, Y_G, and α_G. As the shield displaces into the room, the cables will deform elastically. This deformation, as well as the cable force, will increase until the plastic springs begin to crush. Once crushing occurs, the cable forces remain constant and the crushable material deforms uniformly and plastically.

In the elastic range of response, the total tension force in the top cables, T_1, and the total tension force in the bottom cables, T_2, are derived from the initial and displaced shield geometry (Figure 3.2) and the known stress-strain properties of the cables.

$$T_1 = A_{c1} E_{c1} \frac{[(X_{o1}^2 + h_1^2)^{1/2} - Y_1]}{(X_{o1}^2 + h_1^2)^{1/2}} \tag{3.18}$$

$$T_2 = A_{c2} E_{c2} \frac{[(X_{o2}^2 + h_2^2)^{1/2} - Y_2]}{(X_{o2}^2 + h_2^2)^{1/2}} \tag{3.19}$$

where A_{c1} = sum of the cross-sectional areas of the top cables, in^2.

A_{c2} = sum of the cross-sectional areas of the bottom cables, in^2.

E_{c1}, E_{c2} = modulus of elasticity of the top and bottom cables, respectively, psi

X_{o1}, X_{o2} = horizontal distance from the inside face of the wall to point where the top and bottom cables enter the frame, respectively, in.

h_1, h_2 = vertical distance from the top of the frame to the ceiling and from the bottom of the frame to the floor, respectively, in.

Y_1, Y_2 = deflected length of the top and bottom cables, respectively, in.

The force in the cable cannot exceed the sum of the resisting forces of the springs, $N_s f A_{cm}$, as shown in Figure 3-4. In the plastic range, $f = f_{cm}$ and the maximum forces in the top and bottom cables are:

$$T_1 = N_1 N_{s1} f_{cm1} A_{cm1} \tag{3.20}$$

$$T_2 = N_2 N_{s2} f_{cm2} A_{cm2} \tag{3.21}$$

where N_1, N_2 = number of top and bottom cables, respectively

N_{s1}, N_{s2} = number of springs in each top and bottom energy absorber, respectively

f_{cm1}, f_{cm2} = crushing strength of a single spring in a top and bottom energy absorber, respectively, psi

A_{cm1}, A_{cm2} = cross-sectional area of a single spring in a top and bottom energy absorber, respectively, in^2

By equating the force in the cables to the force in the energy absorbers, the stress in each spring of a top energy absorber, f_1, and a bottom energy absorber, f_2, is:

$$f_1 = \frac{A_{c1} E_{c1} \left[\left(X_{o1}^2 + h_1^2 \right)^{1/2} - Y_1 \right]}{N_1 N_{s1} A_{cm1} \left(X_{o1}^2 + h_1^2 \right)^{1/2}} \tag{3.22}$$

$$f_2 = \frac{A_{c2} E_{c2} \left[\left(X_{o2}^2 + h_2^2 \right)^{1/2} - Y_2 \right]}{N_2 N_{s2} A_{cm2} \left(X_{o2}^2 + h_2^2 \right)^{1/2}} \tag{3.23}$$

The force in the top cables, T_1, is defined by equation (3.18) when $f_1 \leq f_{cm1}$, and is defined by equation (3.20) when $f_1 > f_{cm1}$.

The force in the bottom cables, T_2, is defined by equation (3.19) when $f_2 \leq f_{cm2}$ and is defined by equation (3.21) when $f_2 > f_{cm2}$.

The three dynamic equilibrium equations (3.7) through (3.9) can be solved by using a method of direct integration called the Newmark - β method (Ref 4). The Newmark - β method divides the problem into intervals of time, δt, and performs a step-by-step integration procedure to solve for the displacements, velocities, and accelerations at each time step. The general procedure is as follows:

1. Assume values of the accelerations $\ddot{X}_G$, $\ddot{Y}_G$, and $\ddot{\alpha}_G$ at the end of the time interval.
2. Compute the velocities and displacements at the end of the time interval for each of the degrees of freedom (X_G, Y_G, α_G) using the following equations:

$$V_{n+1} = V_n + (1 - \mu) a_n \delta t + \mu a_{n+1} \delta t$$

$$X_{n+1} = X_n + V_n \delta t + (0.5 - \beta) a_n \delta t^2 + \beta a_{n+1} \delta t^2$$

where $\mu = 0.5$ and $\beta = 0.25$. The terms a_{n+1}, V_{n+1} and X_{n+1} are the acceleration, velocity and displacement at the end of the time interval and a_n, V_n, and X_n are the acceleration, velocity, and displacement at the end of the previous time step.

3. Solve equations (3.7) through (3.9) for a new set of accelerations ($\ddot{X}_G$, $\ddot{Y}_G$, $\ddot{\alpha}_G$) at the end of the time interval.
4. Compare the computed accelerations with the assumed accelerations. If they are within a given tolerance, go on to the next time step. If not, take the computed accelerations as the assumed accelerations and repeat steps 2 through 4 until the accelerations converge.

Step 1 of the Newmark - β method begins at time $t = t_{im}$ when the displacements, velocities, and the cable forces are known. The accelerations are computed directly from equations (3.7) through (3.9). These accelerations are then used as the assumed accelerations for the next time step, $t = t_{im} + \delta t$. In succeeding time steps, the assumed accelerations are equal to those at the end of the previous time step.

The Newmark - β method is unconditionally stable if $\mu = 0.5$ and $\beta = 0.25$. However, convergence problems do occur if the time step $\delta t > 1.0$ millisecond.

3.2.3 Glazing

Theory for dynamic response of the polycarbonate glazing neglects the response of the steel frame supporting the glazing. This assumption is conservative and introduces only slight error because the glazing typically reaches its maximum deflection before the steel frame has undergone significant deflections.

Consider the glazing to be an elastic plate simply supported on non-moving supports. Assuming a single-degree-of-freedom (S.D.O.F.) model for the plate and summing the forces acting normal to the plate,

$$P_e(t) - R(z) - 2\,p\,\sqrt{K_{Lm}\,K(z)\,m}\;\;\dot{z}(t) = K_{Lm}\,m\,\ddot{z}(t) \qquad (3.24)$$

where $P_e(t)$ = reflected blast overpressure-time history given by equation (3.1), psi

p = percent of critical damping

$K_{Lm} = K_m / K_L$

K_m = mass factor for the equivalent S.D.O.F. model

K_L = load factor for the equivalent S.D.O.F. model

$K(z)$ = elastic stiffness of the glazing at deflection z, psi/in.

m = unit mass of the polycarbonate glazing, $lb\text{-}msec^2/in^3$.

$z(t)$ = displacement relative to frame at center of glazing at time t, in.

Accounting for the tensile membrane and bending behavior of a simply supported, thin plate, the resistance of the glazing, R(z), is (Ref 5):

$$R(z) = \frac{\pi^6 D}{16\,b^4}\left[\, z\,(1+\phi^2)^2 + \frac{3\,z^3}{4\,h^2}\,[(3-\mu^2)\,(1+\phi^4) + 4\,\mu\,\phi^2\,]\right] \qquad (3.25)$$

where z = displacement at center of glazing, in.

h = thickness of glazing, in.

b = length of the short span of glazing, in.

D = flexural stiffness of glazing, $E\,h^3 / 12(1-\mu^2)$, $psi\text{-}in^3$

E = elastic modulus of glazing, psi

ϕ = ratio of short span to long span of glazing

μ = poisson's ratio.

The displacement, velocity, and acceleration of the polycarbonate glazing can be computed at each time step by using the Newmark - β method discussed earlier (Ref 4). In the application of the Newmark - β method, the glazing stiffness, K(z), is estimated by:

$$K(z) = \frac{(R_{n+1} - R_n)}{(z_{n+1} - z_n)} \qquad (3.26)$$

3.3 INTERNAL OVERPRESSURES

A measure of the shield's effectiveness is the reduction caused by the shield in the peak blast overpressures inside the building. The interior blast overpressure, $P_i(t)$, is (Ref 6):

$$P_i(t) = P_{so}(t) \left[0.65 \ (R / D)^{-1.35} \right] \qquad (3.27)$$

where $P_{so}(t)$ = the incident blast overpressure outside the building at time t, psi

R = horizontal distance from shield to the point of interest inside room, in.

$D = (a \ b)^{1/2}$, no shield over window opening, in.

$D = [2 \ X_G(t) \ (a + b)]^{1/2}$, with shield over window opening, in.

a = height of window opening, in.

b = width of window opening, in.

$X_G(t)$ = horizontal displacement at mid-height of the shield at time t, in.

3.4 ANCHORS

As shown in Figure 2-8, the cables are anchored to the floor and ceiling by attaching the ends of the cables to a bearing plate. In the case of a concrete slab, the maximum allowable cable force, F_c, based on the allowable shear capacity of the slab (Ref 7) is:

$$F_c = \phi \ 4 \sqrt{f'_c} \ b_o \ d \qquad (3.28)$$

where ϕ = 0.85 = ACI strength reduction factor for shear

f'_c = ultimate compressive strength of concrete, psi

d = effective depth of slab, in.

b_o = effective perimeter of the bearing plate, equal to the plate perimeter plus 3d, in.

3.5 COMPUTER PROGRAM

The program SHIELD has been developed to analyze the response of a safety window shield to an external explosion (Ref 8). The program is

written in FORTRAN 77 and can be executed on any computer that has a FORTRAN compiler. The program computes the following:

- Blast overpressure outside building
- Displacements, velocities, and accelerations of shield
- Displacement of polycarbonate glazing relative to frame
- Forces in top and bottom cables
- Blast overpressure at point five feet above the floor and any distance inside the room
- Strains in crushable springs
- Displacements, velocities, and accelerations of the glass window

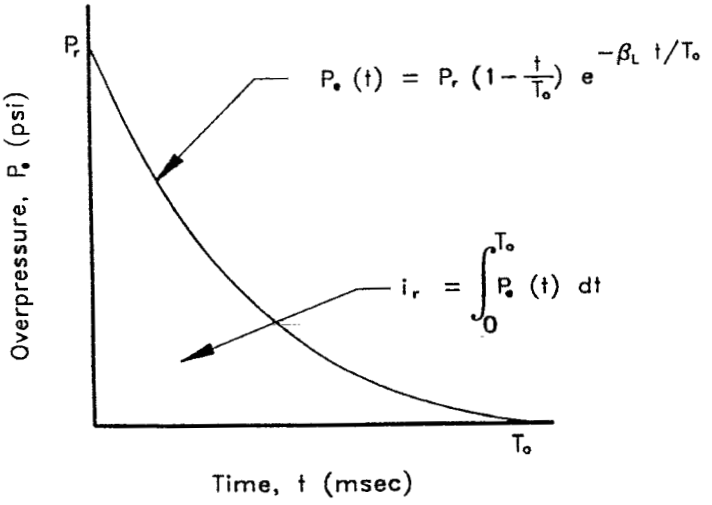

Figure 3-1. Blast load applied to shield.

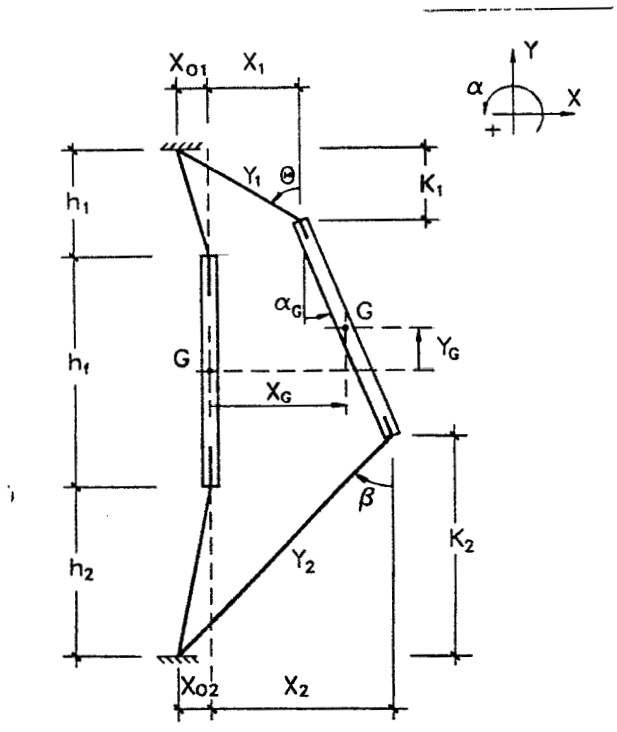

Figure 3-2. Definition of geometric parameters for displaced shield.

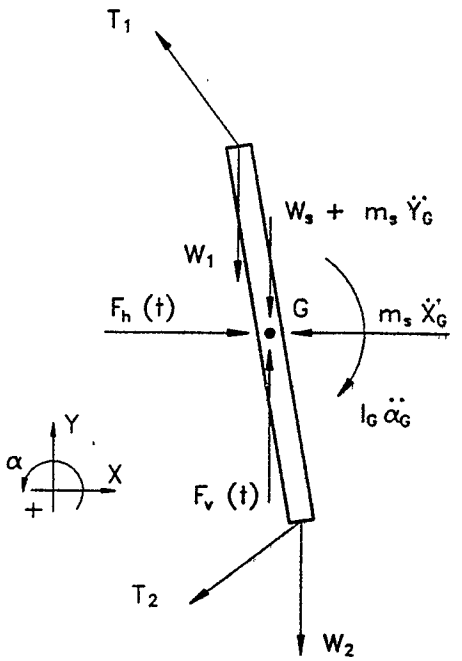

Figure 3-3. Free body diagram of shield.

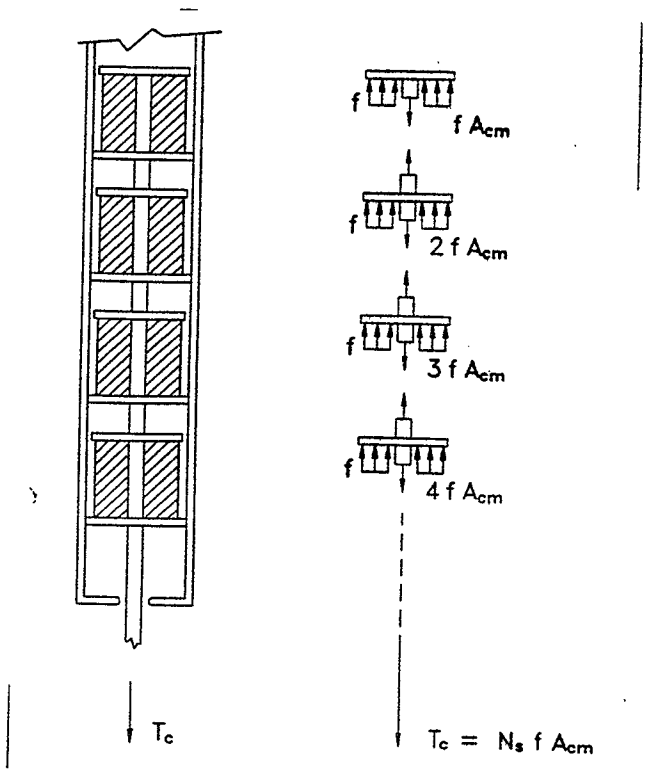

Figure 3-4. Forces applied to energy absorber.

4.0 DESIGN EXAMPLE

4.1 PROBLEM DEFINITION

4.1.1 Explosive Threat

The window is exposed to the blast environment from the detonation of a 1000 pound TNT hemispherical charge. The explosion is a surface burst located 100 feet from the face of the building. According to the NAVFAC P-397 Manual (Ref 1), the maximum reflected overpressure is 24 psi and the duration of the positive pressure phase is 26 msec.

4.1.2 Window Characteristics

The window opening is 6'-0" high and 3'-6" wide. The bottom of the opening is three feet above the floor. The top of the opening is two feet below the ceiling. The window glazing is a single panel of 3/16 inch glass coated with a security film. The air gap between the glass and the shield is 4 inches.

4.1.3 Performance Objectives

The maximum allowable overpresssure inside the room at a point located 8 feet behind the shield is 1.2 psi. The maximum allowable displacement of the frame into the room is 12 inches. Safety from debris and fragments is not considered in this design example.

4.2 SHIELD DESIGN

4.2.1 Glazing

The shield glazing is 3/8 inch thick polycarbonate. The polycarbonate has a yield stress of 9,500 psi, a modulus of elasticity of 345,000 psi, and a rupture strain of 80 percent.

4.2.2 Frame

The frame is made up of 4-inch by 4-inch AISC steel tube sections with a wall thickness of 3/16 inches. The total frame weight is 249 pounds.

4.2.3 Cables

The cable diameter is 1/2 inches. The cables have an allowable design stress of 100,000 psi and an elastic modulus of 13×10^6 psi. The lengths of the top and bottom cables are 2'-0" and 3'-0", respectively.

4.2.4 Energy Absorbers

Each energy absorber consists of one block of aluminum honeycomb, 4 inches in height with a cross sectional area of 10 in^2. The crushing strength of the material is 2052 psi. The maximum allowable strain of the honeycomb material is 70 percent.

4.2.5 Ballast

The top and bottom rails each contain 50 pounds of ballast in the form of lead beads.

4.3 PREDICTED PERFORMANCE

4.3.1 Displacements

Figure 4-1 shows the time history of the external blast overpressure, the displacements at the top, bottom and mid-height of the shield, and the displacements at the center of the glazing relative to the frame. At time t = 4 msec after the blast wave reaches the building, the glass shards and blast wave strike the shield. The shield continues to displace after the end of the loading phase and reaches a maximum displacement of 11.7 inches at time t = 39 msec. This displacement is less than the allowable and occurs at the bottom rail where the restraining cables are the longest. Note that the polycarbonate glazing reaches a maximum displacement of 4.3 inches before the blast overpressure has decayed to zero and long before the frame has reached its maximum displacement.

4.3.2 Internal Overpressure

Figure 4-2 shows the time history of the internal overpressures with and without the shield at points 4 and 8 feet inside the room. The maximum internal overpressure at 8 feet is 1.9 psi without the shield. With the shield in place, however, the maximum overpressure is 0.3 psi. Therefore, the shield reduces the internal blast overpressure by 84 percent, well below the allowable 1.2 psi.

4.3.3 Anchor Force

The maximum anchor force needed to restrain the cables depends on the response of the energy absorbers. For an energy absorber with one spring, the maximum cable force is the cross-sectional area of the crushable material multiplied by its crushing strength. In this example, the maximum cable force is F_c = 2050 psi x $10 in^2$ = 20,520 pounds in each cable. For a 6-inch concrete slab, this requires a 4 by 8 inch anchor plate to limit the shear stress in the slab.

4.3.4 Effectiveness

The shield reduces the peak blast overpressure at a point 8 feet inside the room from 1.9 psi to 0.30 psi, or 84 percent. This reduction in overpressure demonstrates the effectiveness of the shield in ensuring the life safety of inhabitants.

4.4 PARAMETER SENSITIVITY

4.4.1 Ballast

Shield performance is improved by adding ballast to the top and bottom rails of the frame. Figure 4-3 shows the effect of ballast on the maximum shield displacement and peak blast overpressure inside the room.

4.4.2 NRA Factor

The NRA factor is equivalent to the maximum cable force and is defined as the product of the number of blocks of crushable material, N, the resistance or crushing strength of the material, R, and the cross sectional area of the material, A. Figure 4-4 shows the effect of the NRA factor in controlling displacements. It should be noted that the maximum internal pressures are not effected by the NRA factor because the peak overpressure inside the room typically occurs long before the springs begin to crush.

4.4.3 Explosive Weight

The shield can effectively defeat the threats from explosions for a broad range of explosive weights. As shown in Figure 4-5, the shield maintains a high level of effectiveness in reducing the peak blast overpressures inside the room for bomb weights up to 2000 pounds TNT for a fixed standoff distance of 100 feet from the building.

4.4.4 Air Gap

The air gap between the safety window shield and the glass window will vary depending on the building wall thickness and the location of the glass window. Figure 4-6 shows the internal peak blast overpressures at a point 8 feet inside the room for air gap distances ranging from 0 to 40 inches. Note that the internal peak blast overpressure is reduced dramatically in thick-wall buildings that provide large air gap distances.

4.4.5 Anchor Detail

The energy absorber constant or NRA factor dictates the maximum cable force. Figure 4-7 shows the maximum value of the NRA factor to prevent shear failure in a reinforced concrete slab, as a function of slab thickness and anchor plate dimensions.

4.4.6 Number Windows

Figure 4-8 shows the blast overpressure-time history inside a room with 1 to 4 windows. This figure illustrates the capability of the shield to limit the blast overpressures in rooms with multiple windows.

4.5 PROTOTYPE DESIGN

4.5.1 Design Drawings

A typical prototype design for a safety window shield is shown in Figures 4-9 through 4-13. This particular design will be used to test and evaluate the window shield concept and to validate design criteria and computer programs.

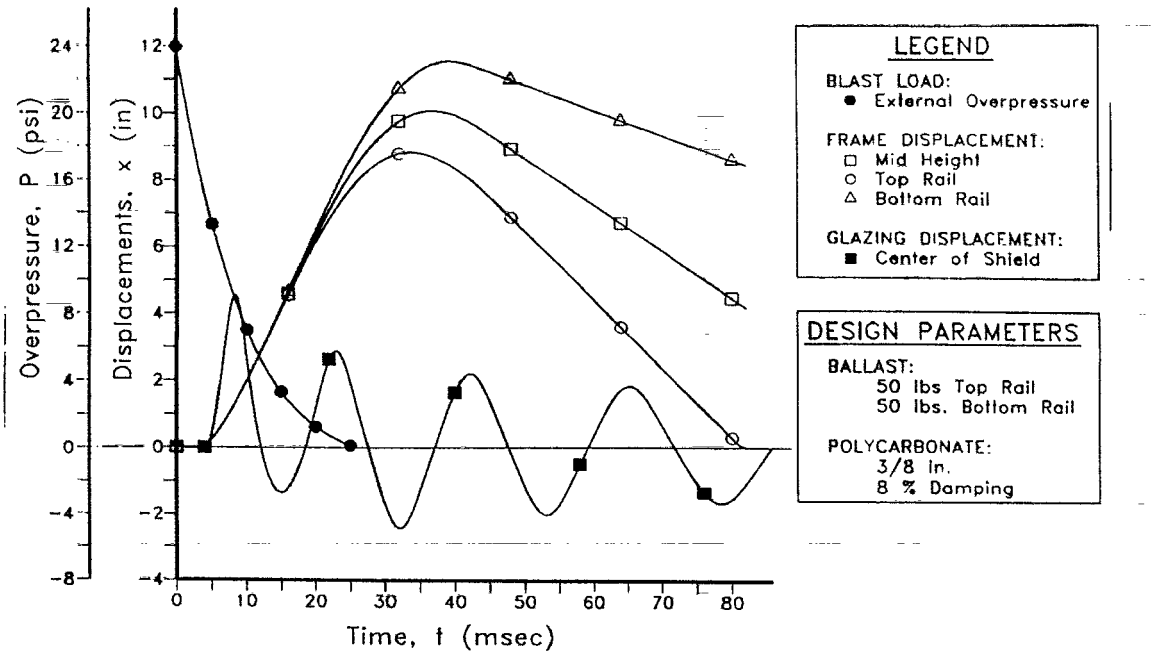

Figure 4-1. Time history of external blast pressure and displacements of frame and glazing.

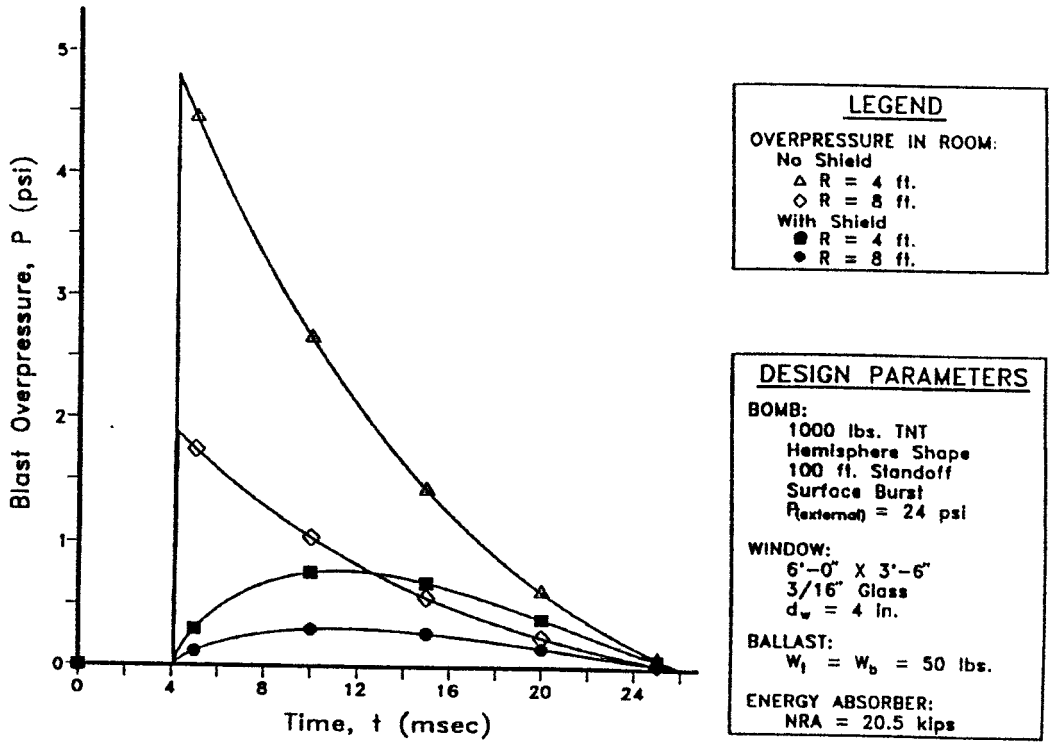

Figure 4-2. Time history of blast pressures inside room with and without shield.

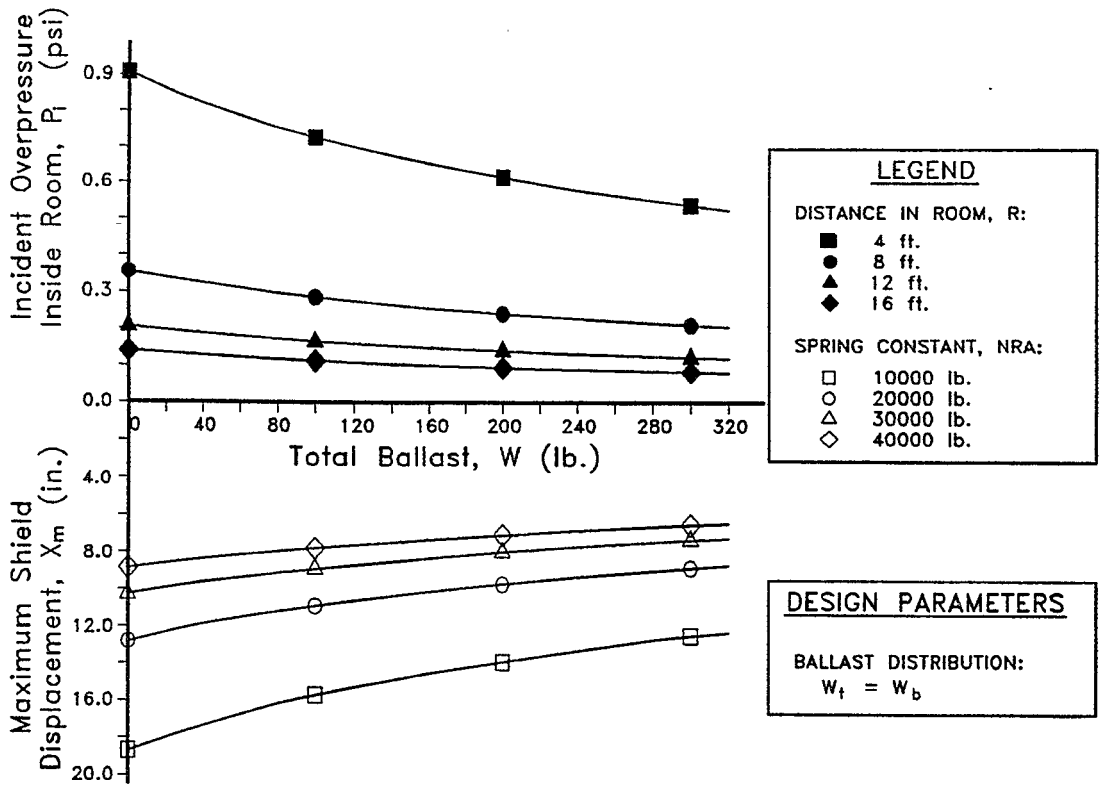

Figure 4-3. Effect of ballast on maximum shield displacements and peak room pressures.

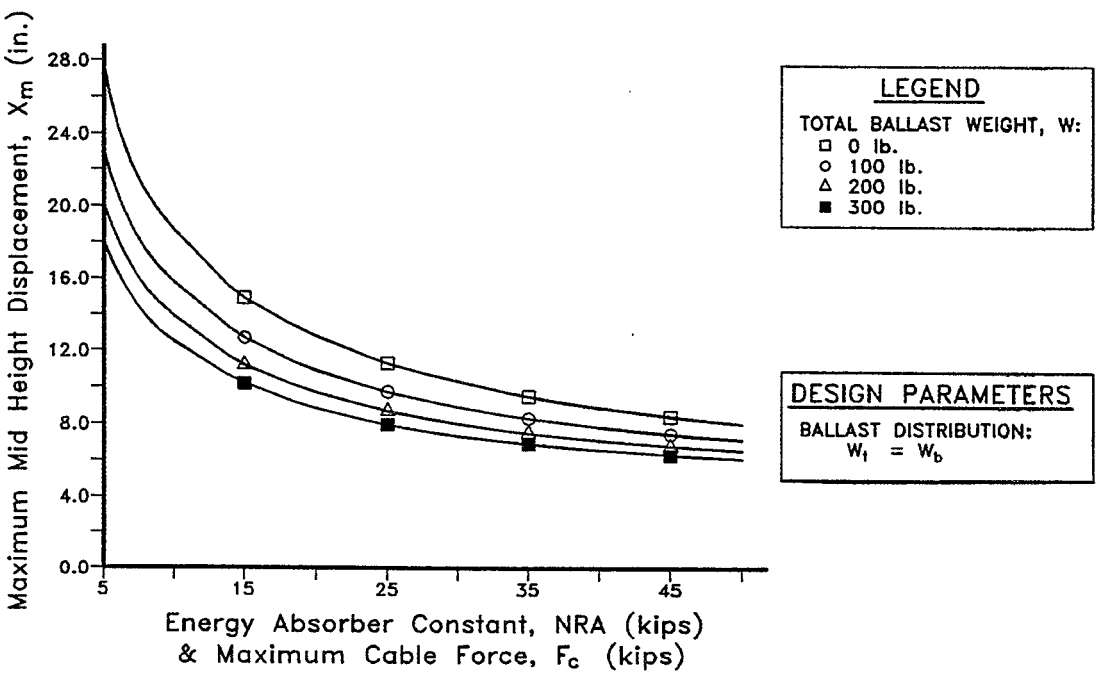

Figure 4-4. Effect of energy absorber characteristics on maximum shield displacement.

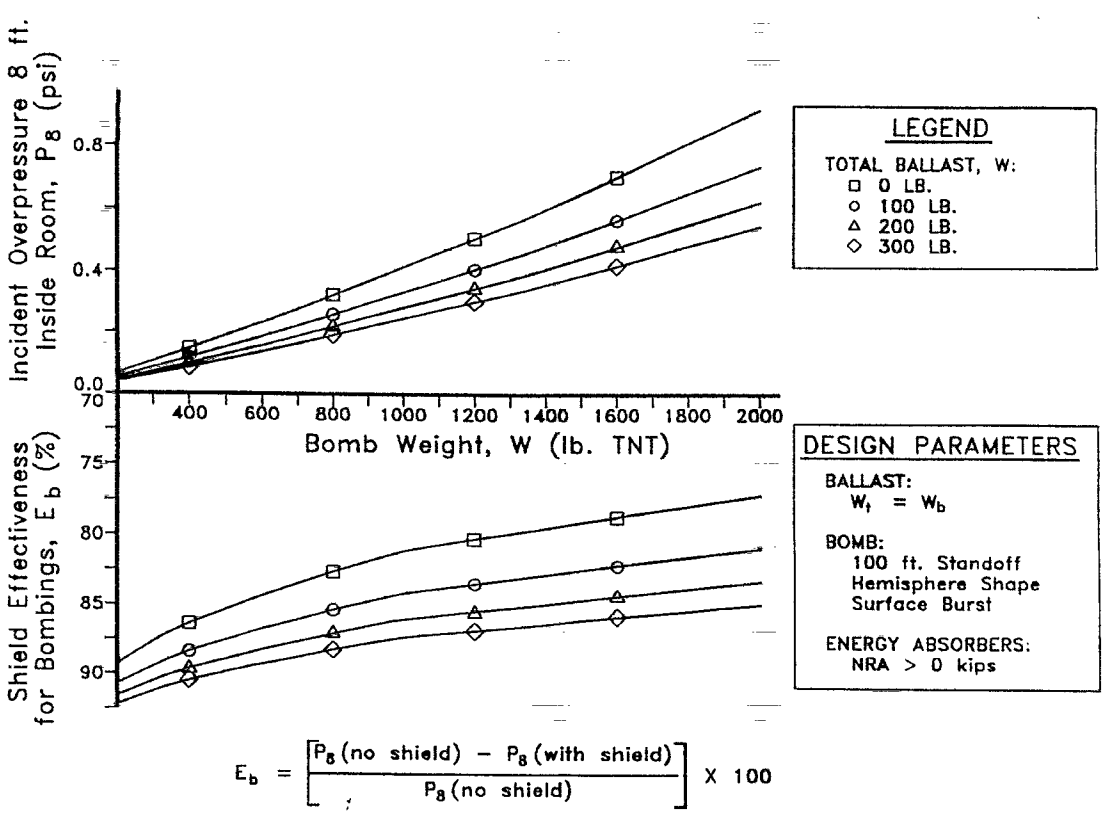

Figure 4-5. Effect of explosive weight on peak room pressures and maximum shield displacements.

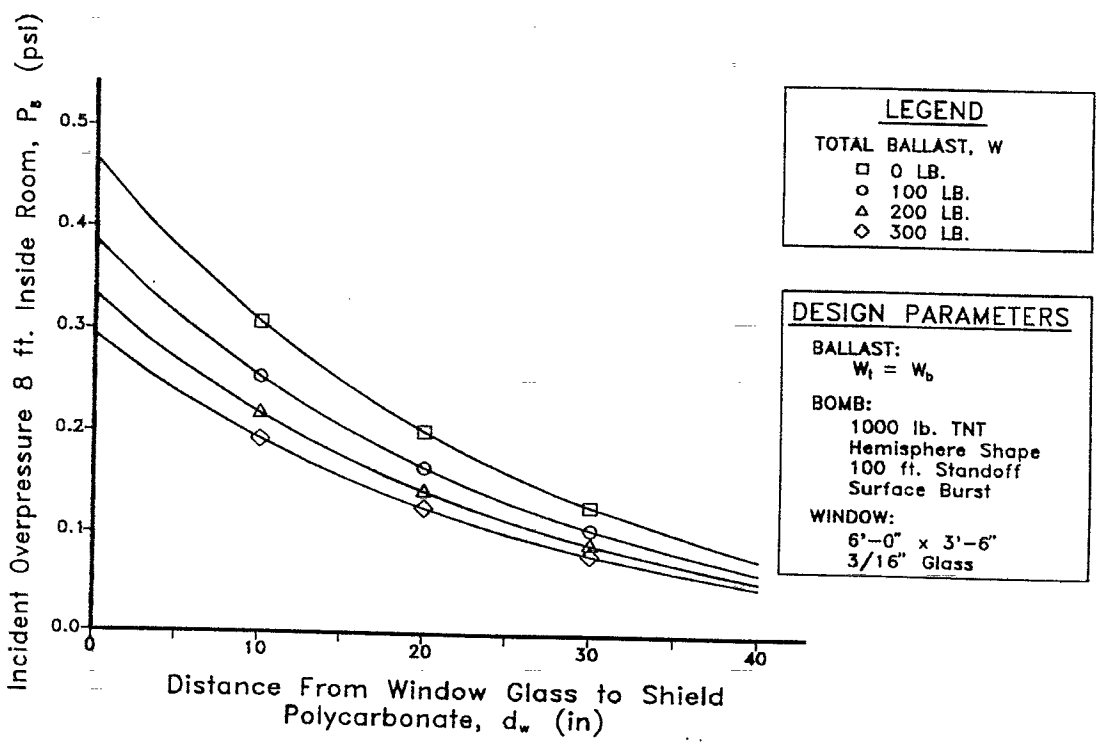

Figure 4-6. Effect of air gap distance between window and shield on peak room pressures.

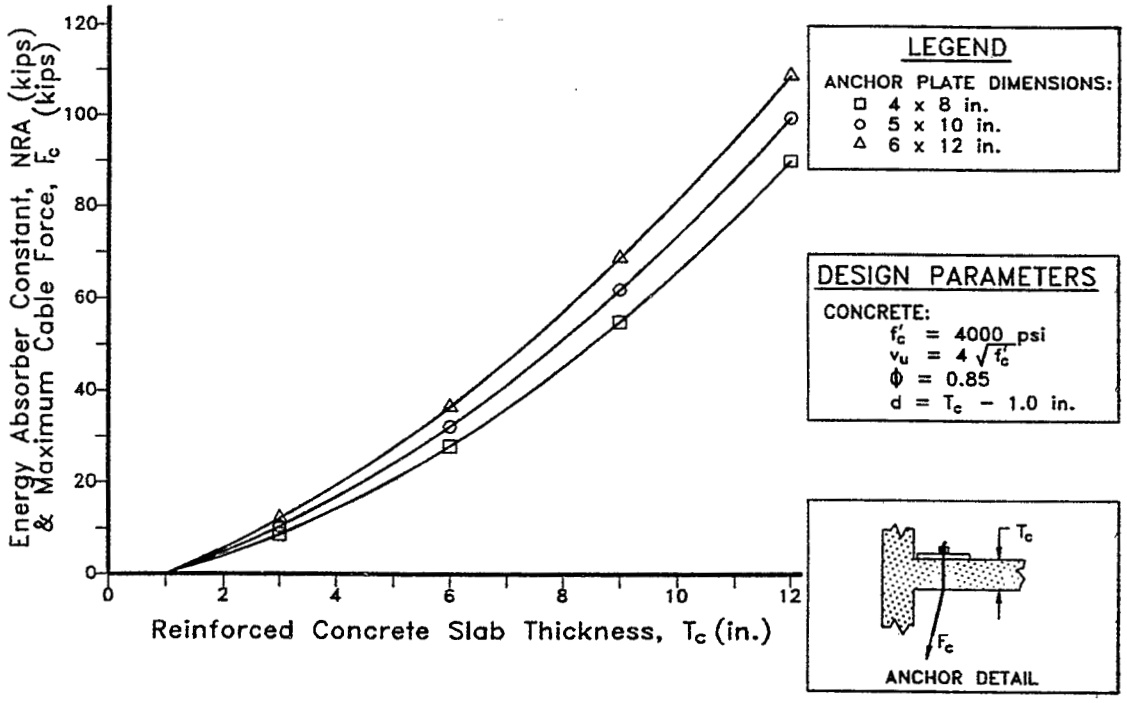

Figure 4-7. Effect of anchor plate dimensions and slab thickness on capacity of cable anchors.

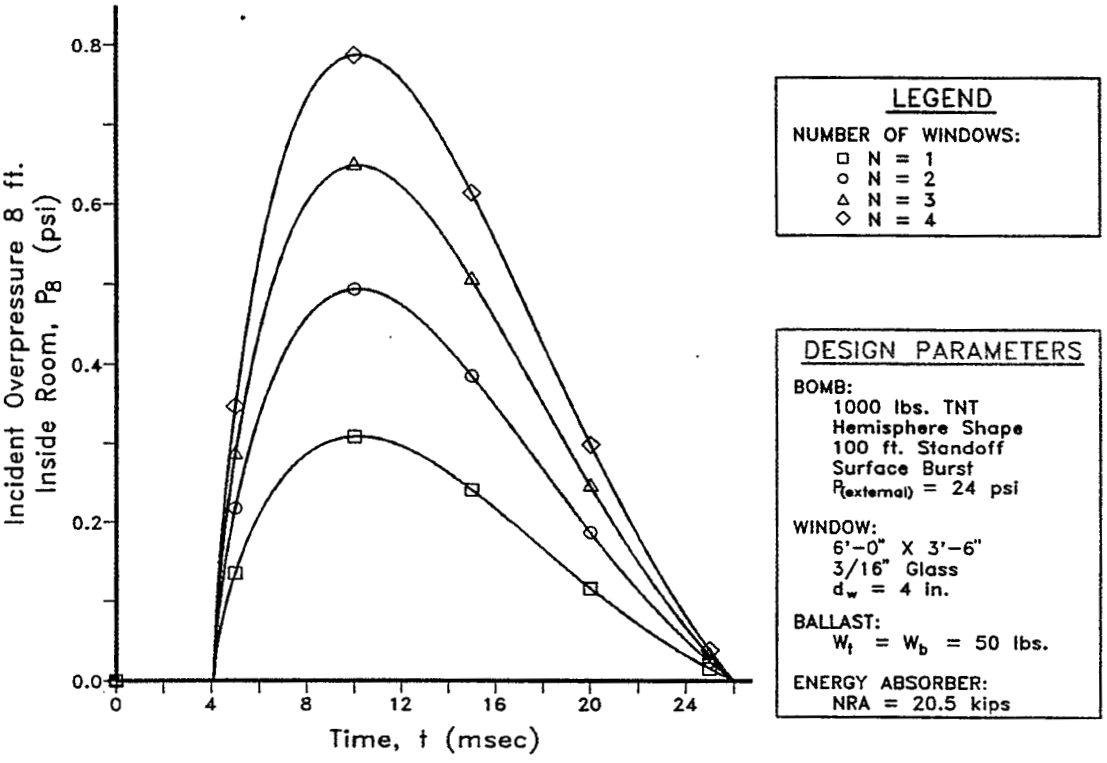

Figure 4-8. Effect of number of windows on room pressures.

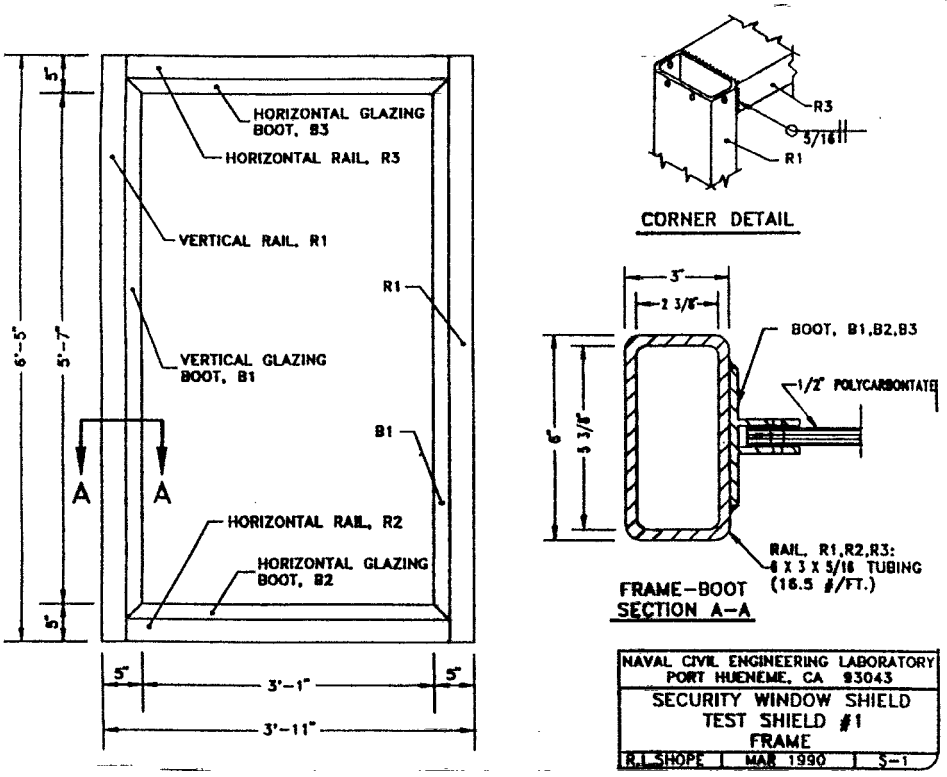

Figure 4-9. Prototype design - frame details.

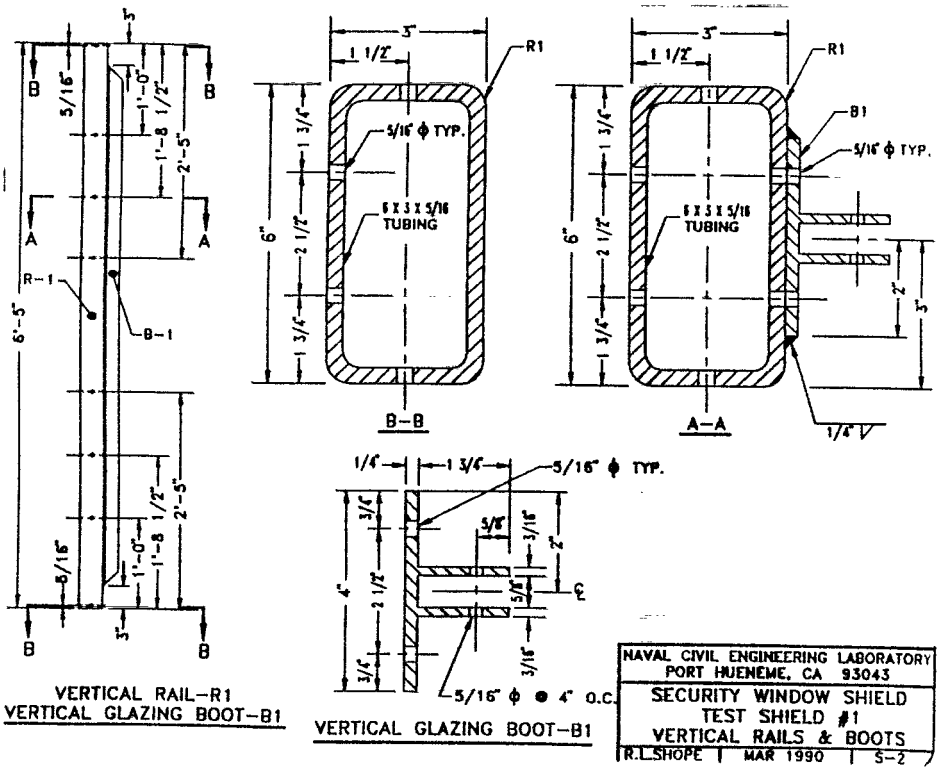

Figure 4-10. Prototype design - vertical rails and boots.

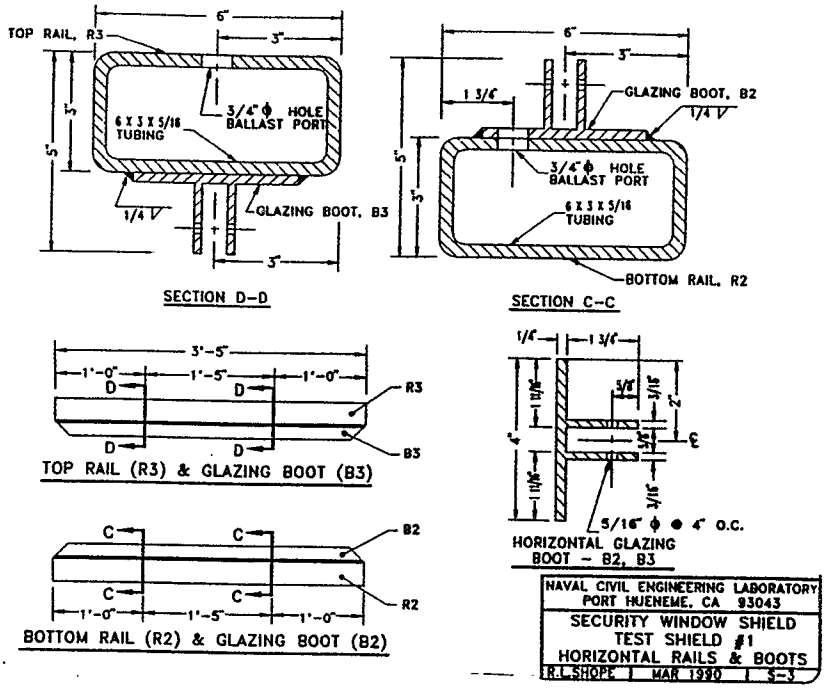

Figure 4-11. Prototype design - horizontal rails and boots.

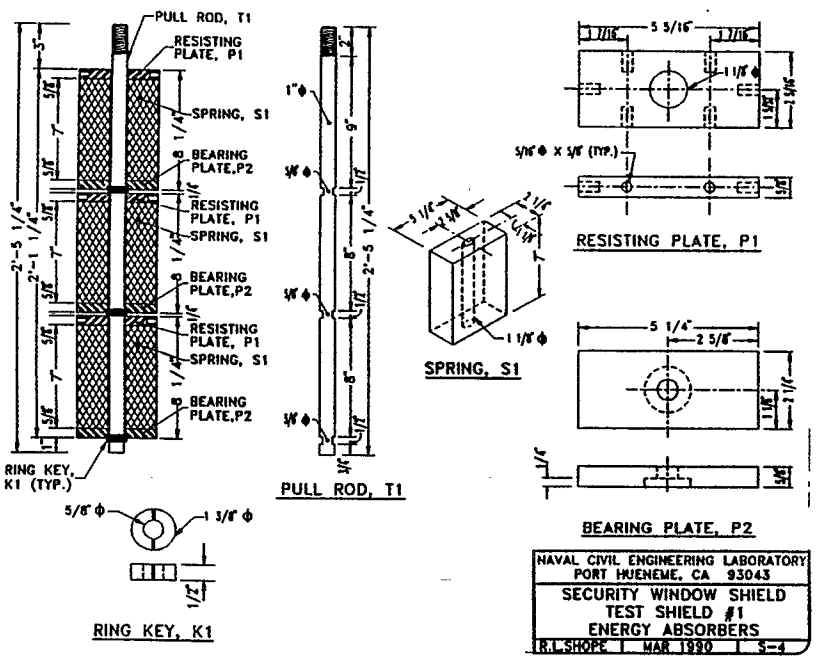

Figure 4-12. Prototype design - energy absorbers..

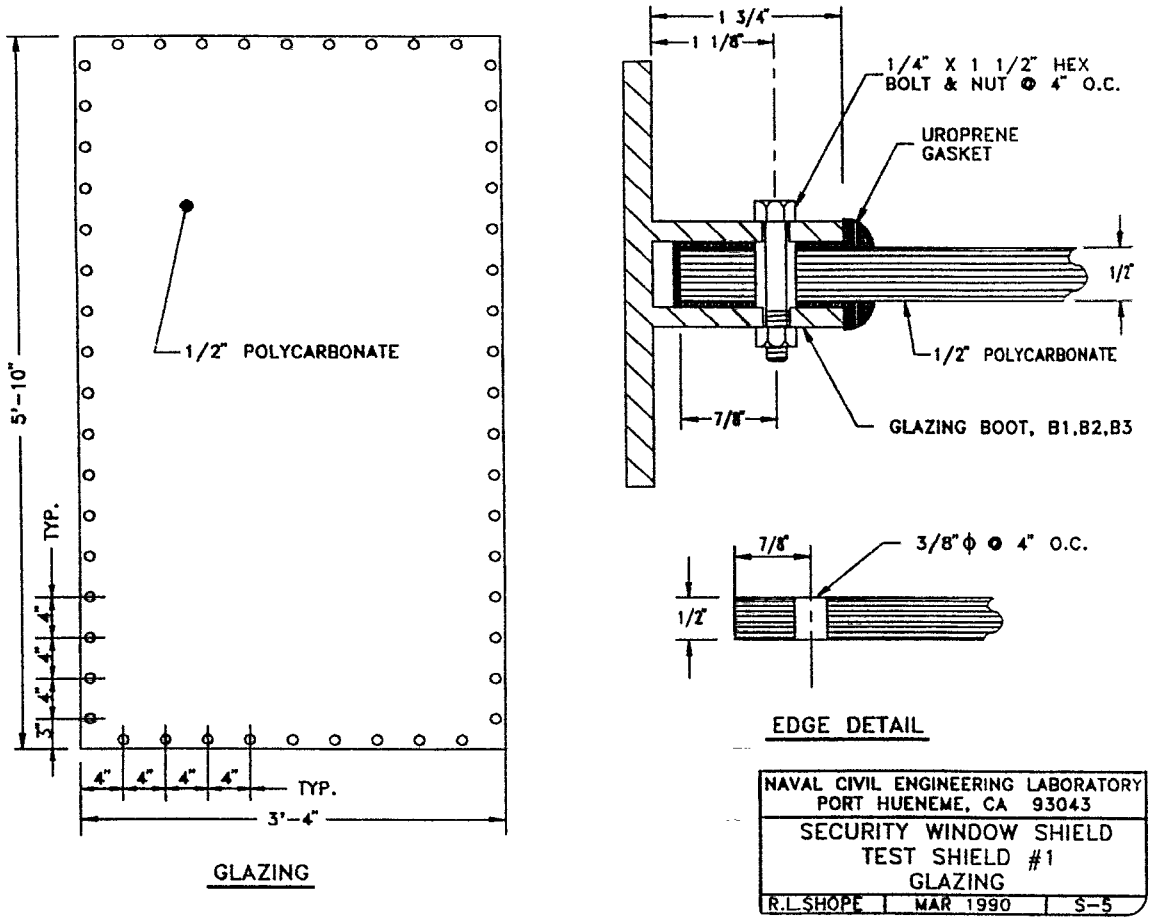

Figure 4-13. Prototype design - polycarbonate glazing.

5.0 BENEFITS

5.1 LIFE SAFETY

The shield substantially improves the safety of inhabitants against glass shards, bomb fragments, debris, and blast overpressures. The concept is universally applicable to any size explosion and window opening.

5.2 LOW COLLATERAL DAMAGE

The shield provides a major reduction in collateral building damage and the probability of structural collapse from an explosion outside the building by transferring applied window loads to the wall-ceiling and wall-floor joints where the building is inherently strong.

5.3 RAPID AND SIMPLE TO INSTALL

The shield is installed by merely drilling four holes (two in the ceiling and two in the floor) and attaching standard cable terminals. The existing window and surrounding wall remain undisturbed.

5.4 UNIVERSALLY APPLICABLE

The shield can be installed in both new and existing buildings made from any type of construction, such as concrete, steel, and masonry.

5.5 ACCOMMODATE CHANGES IN THREAT LEVEL

After the shield is installed, it can be upgraded to accommodate a higher threat level. In addition to permanent deployment, the shield can be quickly installed and removed to offer protection against fluctuating threat levels encountered at U.S. facilities worldwide.

5.6 LOW ACQUISITION AND MAINTENANCE COSTS

Since the shield is made up entirely of commercially available components and installation requires no changes to the existing wall or window, it is an economical alternative to blast "hardened" windows. Also, there are no special or unique maintenance duties to be performed on the shield.

6.0 DEVELOPMENT PLAN

6.1 WORK BREAKDOWN STRUCTURE

Development of the safety window shield is divided into six phases: Conceptual Design, Feasibility Analysis, Test and Evaluation, Prototype Design, Pilot Deployment, and Acquisition. The work breakdown structure for each phase is shown in Figure 6-1.

6.2 CURRENT STATUS

The Conceptual Design and Feasibility Analysis phases, as well as portions of the Test and Evaluation phase, are completed, as shown in Figure 6-1.

7.0 REFERENCES

1. Naval Facilities Engineering Command. NAVFAC P-397 Manual: Structures To Resist the Effects of Accidental Explosions, Vol.II: Blast, Fragment, and Shock Loads, December, 1986, p.31.

2. U.S. Army Corps of Engineers, Design of Structures to Resist the Effects of Atomic Weapons, EM 1110-345-413, July, 1959, p.15.

3. Hornbeck, R.W., Numercial Methods, Prentice-Hall, Englewood Cliffs, New Jersey, 1975, pp.65-66.

4. Newmark, N.M., "A Method of Computation for Structural Dynamics," American Society of Engineers, Vol 127, Part I, 1962, pp.1406-1435.

5. Bares, R., Tables for the Analysis of Plates, Slabs, and Diaphrams Based On Elastic Theory, Bauverlag, Wiesbaden, Germany, 1969, pp.501-507.

6. Drake, J.L. and J.R. Britt, "Propagation of Short Duration Air Blast Into Protective Structures," Proceedings of the Second Symposium on the Interaction on Non-Nuclear Muntions With Structures, Panama City Beach, FL, April,1985.

7. American Concrete Institute, "Building Code Requirements for Reinforced Concrete," ACI 318-83, Detroit, MI, 1984.

8. Naval Civil Engineering Laboratory, Technical Memorandum TM-51-90-17 "Theory and User's Manual: Computer Program for Dynamic Response of a Security Window Shield," R.L. Shope and J.R. Bogle, Port Hueneme, CA, September 1990.

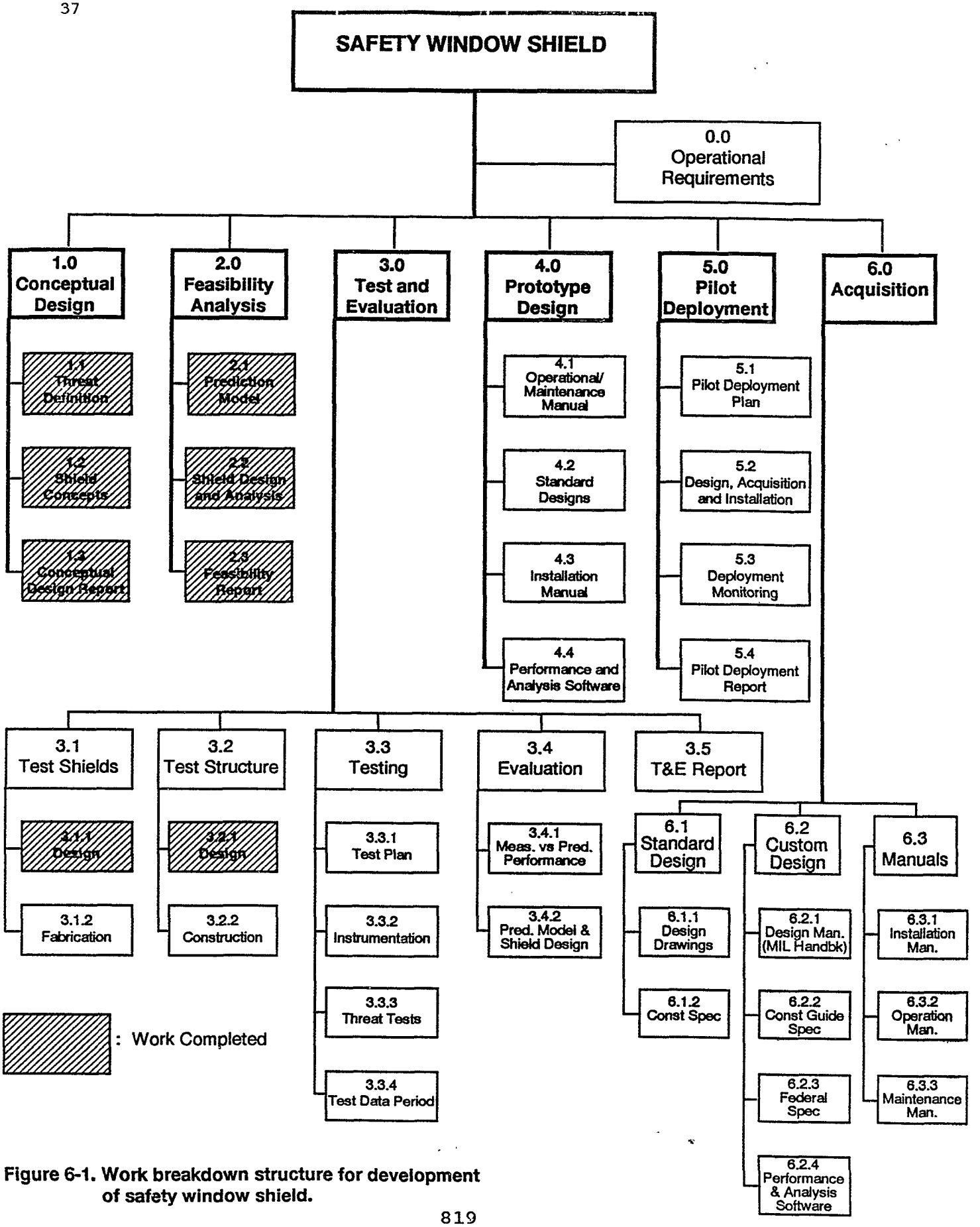

Figure 6-1. Work breakdown structure for development of safety window shield.